Materials Letters 213 (2018) 27–30

Contents lists available at ScienceDirect

Materials Letters

journal homepage: www.elsevier.com/locate/mlblue

Spinel $MgFe_2O_4$ thick films: A colloidal approach for developing gas sensors

Jayvant Patil [a], Digambar Nadargi [a], Imtiaz S. Mulla [b], S.S. Suryavanshi [a,*]

[a] *Department of Physics, School of Physical Sciences, Solapur University, Solapur 413255, India*
[b] *Emeritus Scientist, Centre for Materials for Electronics Technology, Pune 411008, India*

ARTICLE INFO

Article history:
Received 26 September 2017
Received in revised form 27 October 2017
Accepted 2 November 2017

Keywords:
Sensors
Sol-gel preparation
Thick films
Semiconductors
Nanocomposites

ABSTRACT

We report a facile synthesis of spinel $MgFe_2O_4$ thick films and their use as gas sensors via sol-gel process. The choice of reductant (citrate) in combination with oxidizers (metal nitrates) led to exothermic self-sustaining anionic redox reaction of xerogel. Gas sensing properties are described using an interplay of interfacial colloidal chemistry, structural and morphological properties of the developed material.

1. Introduction

The fabrication of advanced spinel ferrite based systems is an active area of research due to their utility in wide applications such as biomedical and electronics, magneto-electric composites, high density magnetic and radar absorbing materials, catalytic activities as well as gas and humidity sensing devices [1–5]. To obtain such multifunctional hybrid composites one of the simplest and commonly exploited strategies is sol-gel hybridization, which allows enhanced control over homogeneity, elemental composition and morphology of the final compound. Since the pioneering work of Hans Goldschmidt on ferrite nanocomposites, several types of MO/Fe_2O_3 mixed-oxide ferrites have been reported [6]. These are mostly cubic ferrites, crystallized into spinel structure with spinel lattice composed of 32 close packed oxygen arrangement as a unit cell. In the state-of-art, these materials claimed various synthetic strategies such as solid-state ceramic sintering, microemulsion, double-sintering and co-precipitation techniques [7–10]. Ravinder et al. reported nano-structured magnesium-chromium ferrites synthesized by citrate-gel autocombustion method, where superparamagnetic behavior of $MgCr_xFe_{2-x}O_4$ nano ferrites are discussed [11]. Deganello et al. reported citrate-gel autocombustion route for developing the perovskites of iron, cobalt and cerium [12]. However, to the best of our knowledge, little-to-no work has been carried out for the synthesis of Mg-ferrites by citrate-gel-combustion method [13]. The citrate-gel method is a simple sol-gel process, which offers advantage over the traditional approach due to better dispersion and versatility when it comes to the synthesis of multicomponent mixed ferrite materials. As the citric acid is widely used acidulent to form a gel, the viscosity of the precursor solution/sol shoots up with increasing temperature by the addition of citric acid. Finally, the gelly state is attained (Fig. 1a): Graph part) due to specific chemical nature of weak acid, weak bonding of Cl^- or NO_3^- of metal salts and water ligands in the metal coordination shell as leaving groups. In the present work, we demonstrate a facile and flexible strategy for fabricating spinel $MgFe_2O_4$ thick films via citrate gel combustion process, and their use as gas sensor for various reducing gases.

2. Experimental and sol-gel process

In a typical synthesis, metal nitrates ($Mg(NO_3)_26H_20$, $Fe(NO_3)_39H_20$) and citric acid ($C_6H_8O_7$) were used as-received (Reagent-grade, S.D.fine chemicals). Stoichiometry of the redox mixture for combustion was calculated on the basis of total oxidizing and reducing valence of oxidizer and reductant (3:5 mol). The calculated quantities of nitrate salts were dissolved in double-distilled water followed by the addition of required amount of citric acid. The reaction mixture/sol was stirred for ample time, till it attained the homogeneous phase. The temperature of sol was eventually raised up to 425 K. In accordance with the natural behavior

---

* Corresponding author.
E-mail address: sssuryavanshi@rediffmail.com (S.S. Suryavanshi).

https://doi.org/10.1016/j.matlet.2017.11.009

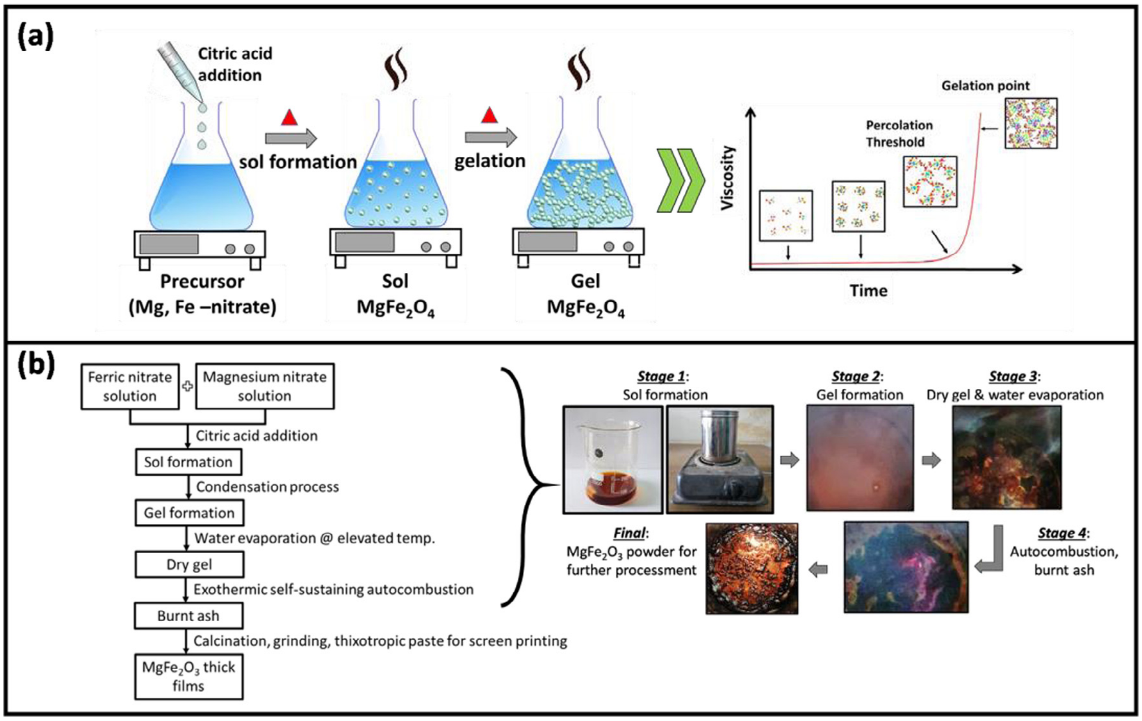

Fig. 1. (a) Schematic illustration for the preparation of ferrite gel, using citrate initiated sol-gel process. (b) flow of complete synthetic protocol and their corresponding pictorial stages.

(Fig. 1a), at the set temperature the sol viscosity increased gradually with certain time. During this period, the sol became highly viscous. After attaining percolation threshold, the viscosity increased exponentially without the presence of liquid state. In other words, gel state with enriched water was achieved. The resultant gel was continued to heat treat at bit higher temperature (450–475 K). The viscous gel began frothing and eventually after water evaporation, the gel started exhausting into fast flameless auto combustion reaction with the evolution of large amount of gaseous products. The porosity of the gel network was completely collapsed and turned into voluminous $MgFe_2O_4$ xerogel powder (Fig. 1b).

Finally, the xerogel was calcined in air at temperature 775 K for 2 h in order to get rid of unreacted reductant, oxidizers and their decomposition products (if any), and obtained the pure compound. Using screen printing technique, the thick films of as-prepared powder were developed on the alumina substrates. Finally, the films were sintered at two different temperatures (Sample C1: 973 K, Sample C2: 1173 K) for 2 h, to study the characteristic performances.

3. Results and discussion

Fig. 2 depicts the crystallographic and microstructural analyses of as-prepared ferrite material. The XRD pattern is belonging to the spinel structure $MgFe_2O_4$ for both the samples (JCPDS file No. 73–1720). The detailed discussion on crystallographic analysis is made in our earlier work [13], which makes ease to limit ourselves for highlighting the new results in the present communication. The colloidal approach of forming porous network structure is symbolized under SEM and TEM investigations. The material showed porous morphology with some voids and empty spaces. Sample C1 displayed typical porous structure with partially developed rounded grains, whereas fully developed grains with pyramid shape and decreased porosity is observed in sample C2. The average grain size of the samples (C1&C2) was found to be ~0.1 μm and ~0.4 μm, respectively. Due to coarsening behavior during sintering, the grain growth increased. This confirms to classic grain growth kinetics, which is evolved in the morphological images as well [14]. Elemental analysis (EDS) of as-developed-material confirmed the presence of Mg, Fe and O, and thereby the formation of $MgFe_2O_4$ (Table 1).

The sensing proficiency of as-developed materials towards reducing gases (LPG, acetone, ethanol, ammonia) was studied. In case of sample C1 (Fig. 3a), with an increase in the operating temperature, the gas response increased, attained a certain maxima, and then decreased further. The curve for ammonia in the range of 500–550 K, was mainly induced by the adsorption and desorption of oxygen molecules from the surface of the sensor film. On exposure to ammonia, oxygen molecules chemisorbs in the form of O_2^-, O^- and O^{2-}. Therefore, more electrons release into the conduction band of ferrite, resulting in the higher variation in the resistance and the distorted response [15]. In contrast, for the sample sintered at higher temperature (Fig. 3b, C2), a gradual increase in the gas response was observed with increasing operating temperature up to 725 K. This articulates the high dependency of sensors' response on the material's sintering temperature [16]. The lower sintered sample has more porous structure, enhancing the higher surface area and thereby better gas-response property. However, due to higher sintering, the materials' gas response nature clearly commands an inappropriate candidate for idea gas sensor. Therefore, the response characteristics after 725 K are not entrained further.

At an optimized operating temperature, all the four gases mentioned above were further studied in accordance with gas concentration and sensor response (Fig. 3c, d). The gas response property of both the sensors was found to increase linearly with the concentration of test gas due to increased probable interactions of the gas molecules with the available active surface area, and then it start to saturate up to 3000 ppm. Moreover, sensor C2 showed better response than sensor C1. They exhibited the response of (10&18), (46&68), (30&35) and (6&1)% at 100 ppm towards LPG, acetone,